

Coherent population trapping atomic clock by phase modulation for wide locking range

Yuichiro Yano, Masatoshi Kajita, Tetsuya Ido, and Motoaki Hara

Citation: *Appl. Phys. Lett.* **111**, 201107 (2017);

View online: <https://doi.org/10.1063/1.4991560>

View Table of Contents: <http://aip.scitation.org/toc/apl/111/20>

Published by the [American Institute of Physics](#)



Scilight

Sharp, quick summaries **illuminating**
the latest physics research

Sign up for **FREE!**

AIP
Publishing

Coherent population trapping atomic clock by phase modulation for wide locking range

Yuichiro Yano,^{a)} Masatoshi Kajita, Tetsuya Ido, and Motoaki Hara

National Institute of Information and Communications Technology 4-2-1 Nukui-Kitamachi, Koganei, Tokyo 184-8795, Japan

(Received 21 June 2017; accepted 24 October 2017; published online 15 November 2017)

A method of detecting Coherent Population Trapping resonance by phase modulation (PM) was studied to expand the frequency locking range (LR). We calculated error signals by density matrix analysis using an eigenvector algorithm and verified the calculated result using an ^{87}Rb vapor cell and a $\text{Rb-}D_1$ vertical cavity surface-emitting laser. By comparing the error signal for PM with that for conventional frequency modulation (FM), it was found that the LR with PM is one order of magnitude wider than that with FM without degrading the frequency stability. *Published by AIP Publishing.*

<https://doi.org/10.1063/1.4991560>

Microwave atomic clocks using Coherent Population Trapping (CPT) have achieved a highly reproducible frequency reference with small size and low power consumption.¹ It is anticipated that these features will not only lead to replacement of elaborate crystal-based oscillators but also bring the benefit of mobile frequency standards to various applications such as wireless communication, sensor network, and positioning system. Further reduction in power consumption for battery operation is currently pursued in the use of the sleep mode² since the warm-up time is reduced considerably in CPT clocks owing to the immunity of CPT resonance to the change in operation environment.

CPT atomic clocks are realized by tightly stabilizing a local oscillator (LO) to a narrow CPT resonance. While we normally employ voltage-controlled crystal oscillators (VCXOs) as LOs, the deviation of their frequencies from the nominal value is often larger than the spectral width of the CPT resonance, requiring an initial sweep of LO frequency to engage the stabilization. It is critically important to eliminate this initial frequency search for future intermittent operations. Broadening the linewidth of the CPT resonance by high light intensity could be a solution to expand the locking range (LR), but the overall performance suffers from the penalty of lower frequency stability as both the quality factor and signal to noise ratio (SNR) of the resonance degrade because of power broadening and optical pumping. Also, high light intensity leads to the increase in the light shift, which degrades the long-term frequency stability. Tight screening of VCXO or adding a control unit for temperature makes it difficult to provide clocks within the acceptable range of cost, size, and power consumption.

In this study, the phase modulation (PM) method was applied to the detection of the CPT resonance to expand the LR without broadening the linewidth. The PM method was established to detect the resonances in optical systems such as simple two-level systems or optical cavities.^{3–5} The LR using this method can be widened without broadening the absorption peak. The CPT resonance, on the other hand, is a phenomenon that is relevant to an atom with three levels and two incident optical radiations. While the system is quite

different from the two-level system, the CPT resonance can be regarded as an interaction of the two-level system comprising dark and bright states with one microwave photon.⁶ We considered that it is possible to apply the PM method to the CPT resonance similarly to the two-level system in optical spectroscopy. To verify this assumption, an error signal for the stabilization was first simulated on the basis of the density matrix analysis using a modified eigenvector algorithm, resulting in good agreement with the theory of simple two-level systems. The PM method was also applied to the ^{87}Rb CPT atomic clock using a vertical cavity surface-emitting laser (VCSEL). By experimentally comparing the error signal for PM and conventional frequency modulation (FM), we confirmed that the fractional LR (FLR) is expanded from sub ppm to several ppm without degrading the short-term frequency stability.

We improved a simulation program based on a density matrix using a time-domain solution algorithm^{7,8} to deal with the transient response of the CPT resonance numerically. Recently, the time-domain algorithm was reported and verified by another group.⁹ In this improved program, we can take into account the various effects induced by light intensity and relaxation rates, which were impossible to deal with by frequency-domain solution.¹⁰ A Λ -type three-level model of ^{87}Rb having two ground states and a common excited state was adopted in the calculation. The two ground states correspond to $F=1, m_f=0$ and $F=2, m_f=0$ in the $5^2S_{1/2}$ state, and the excited state corresponds to the $5^2P_{1/2}$ state. The total decay rate of $5^2P_{1/2}$ was set to 490 MHz, which we obtained from the absorption lines of a ^{87}Rb cell with N_2 buffer gas at a pressure of 4.0 kPa.¹¹ The error signal of the CPT resonance was generally obtained by a synchronous detection of the transmitted light intensity, which is calculated on the basis of the density matrix analysis. Our developed algorithm gives a solution of the density matrix with modulation. Then, the error signal can be numerically derived by obtaining the Fourier transform of the solution at modulation frequency.

The inset of Fig. 1 shows the dependence of the signal amplitude of the CPT resonance on the modulation frequency $f_{\text{mod}} (= \omega_{\text{mod}}/2\pi)$ calculated using our program. The signal amplitude had a cutoff characteristic when using FM, in

^{a)}Electronic mail: y-yano@nict.go.jp

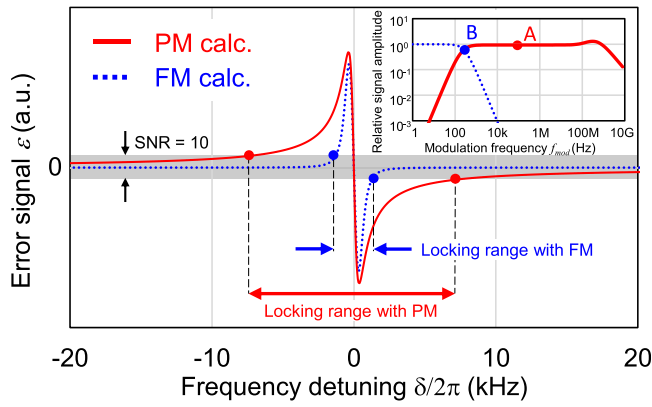


FIG. 1. Numerically calculated error signal of CPT resonance with PM (red solid line) and FM (blue dot line): The gray band shows the noise level in the case of SNR = 10, which determines locking ranges. The inset shows the signal amplitude as a function of modulation frequency. Points A and B for PM and FM are the operating points that we employed in this work. The full width at half maximum of the CPT resonance γ/π is set at 540 Hz.

which the slope of the decrease was -20 dB/dec, owing to the limited linewidth of the CPT resonance. When using PM, the signal amplitude had a band-pass-like characteristic. The signal amplitude increased when f_{mod} was close to the relaxation of ground states $\gamma/2\pi$ and maintained its value up to the relaxation rate of the optical transition $\Gamma/2\pi$. Thus, a high modulation frequency of over $\gamma/2\pi$ can be used to detect the CPT resonance using PM. This means that FM detects the change in the steady states relevant to incoherent processes, which takes a certain amount of decay time. On the other hand, incoherent process is not necessary for PM since it effectively detects the coherent phase shift of one microwave photon. These frequency responses of signal amplitude were experimentally confirmed by our setup as described later.

Figure 1 shows the numerically calculated error signals at the modulation frequency A ($=100$ kHz) and B ($=270$ Hz) in the inset. The horizontal axis is a frequency detuning δ relative to the atomic transition between two ground states. Here, a large error signal was obtained using PM with large detuning ($\delta/\gamma > 1$) even though the slopes for PM and FM overlapped near the transition frequency ($\delta/\gamma \sim 0$). LR can be defined as the frequency range where LO is stabilized to the transition without frequency sweeping. Then, in the case of SNR = 10 where the noise level is indicated as the gray band, we can determine the LR as shown in Fig. 1. It is clearly indicated that PM has wider LR than FM. In addition, note that the slope of the error signal and SNR determine the short-term frequency stability of the atomic clock. Thus, the PM method allows the LR to be expanded without degrading the short-term frequency stability.

By referring to the derivation of the error signals of the two-level system,³⁻⁵ assuming that the CPT resonances approximate the Lorentz function⁶ with a linewidth of 2γ and the modulation frequency ω_{mod} is much larger than γ , the error signals of PM near the resonance with the electric susceptibility χ are expressed as

$$\varepsilon_{PM} \approx -K \operatorname{Re}(\chi) = -K \frac{2\delta\gamma}{\delta^2 + \gamma^2}, \quad (1)$$

where K is a constant depending on the sideband intensity. Assuming that the modulation frequency ω_{mod} is set to be equal to γ , the error signal of FM near the resonance is expressed as

$$\varepsilon_{FM} \approx -K\omega_{mod} \frac{d}{d\delta} \operatorname{Im}(\chi) = -K \frac{2\delta\gamma^3}{(\delta^2 + \gamma^2)^2} = \frac{\gamma^2}{\delta^2 + \gamma^2} \varepsilon_{PM}. \quad (2)$$

Equations (1) and (2) indicate that the error signal has a higher value for PM than for FM in the off-resonance ($\delta/\gamma > 1$) and that the error signals for PM and FM overlap in the on-resonance ($\delta/\gamma < 1$). Note that the error signal decreases at large detuning proportional to $1/\delta$ and $1/\delta^3$ in the PM and FM cases, respectively. The equations are in good agreement with the numerical results shown in Fig. 1. Thus, it was confirmed that the PM method can be applied to the detection of the CPT resonance similarly to the two-level system in optical spectroscopy.

To confirm the broad LR experimentally, a desktop-size atomic clock was constructed as shown in Fig. 2. A single-mode VCSEL (Vixar Inc., P/N: I0-0795S-0000-B005) was employed as a light source. The wavelength of the VCSEL was 795 nm, which corresponds to the $^{87}\text{Rb}-D_1$ line. The VCSEL was driven by a dc injection current of 1.0 mA and an RF signal whose frequency was half of the clock transition frequency. The frequency or phase of the RF signal is modulated synchronously with the modulation frequency f_{mod} by using FM and PM functions of the RF generator. The phase modulation depth is set at 0.8 rad. The laser wavelength was locked to the Rb absorption line by controlling the temperature and injection current. The laser was circularly polarized. The output power of the signal generator, the light power incident on the cell, and the beam diameter were set to -11.2 dBm, $16 \mu\text{W}$, and 3 mm, respectively. Isotope-enriched ^{87}Rb atoms and N_2 buffer gas were sealed in a glass cell of 25 mm diameter and 22.5 mm length. The pressure of the mixed gas was 4.0 kPa. The cell was covered with a solenoid coil to control the bias magnetic field. The temperature of the gas cell was maintained at 60.0°C . The light passing

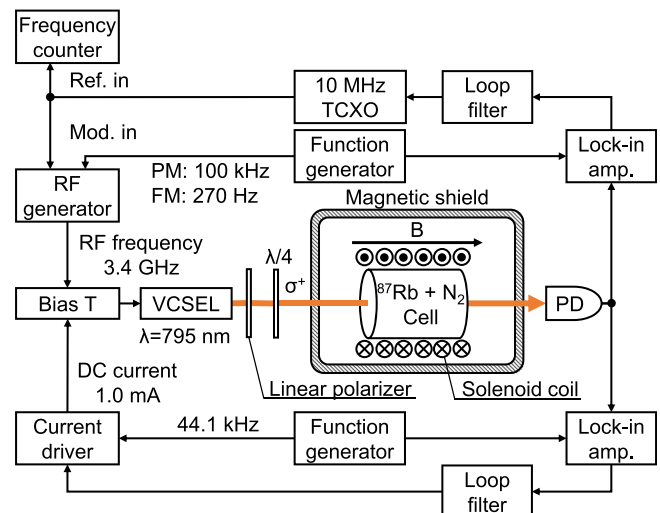


FIG. 2. Schematic diagram of the atomic clock used in the experiment. PD: photodetector and TCXO: temperature-compensated crystal oscillator.

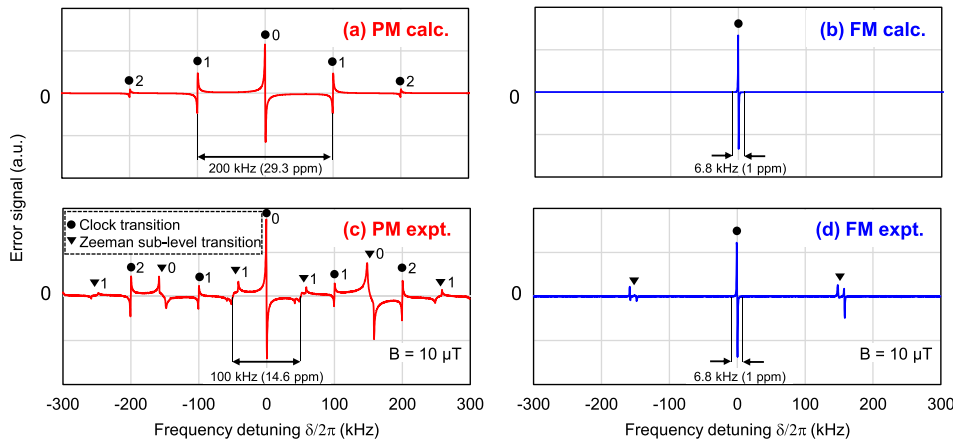


FIG. 3. Error signals with PM and FM: (a) calculation result with PM when a bias magnetic field of $10 \mu\text{T}$ is applied, (b) calculation result with FM, (c) experimental result with PM, and (d) experimental result with FM when a bias magnetic field of $10 \mu\text{T}$ is applied.

through the gas cell was measured with a photodetector. A temperature-compensated crystal oscillator (TCXO) was employed as an LO. The output frequency was measured by a frequency counter which was referenced by a hydrogen maser. The clock frequency was found to be $6.834,696,636 \text{ GHz}$ by observing the CPT resonance. This value was 14 kHz higher than that of the ^{87}Rb fountain clock.¹² This shift was caused by the N_2 buffer gas.

The experimental results are shown in Fig. 3 along with calculated results. The measured SNR of resonance was about 700 in this experiment. Several undesirable peaks indicated by filled triangles (\blacktriangledown) can be observed in Figs. 3(c) and 3(d). These peaks correspond to Zeeman sublevels. By tuning the bias magnetic field, the positions of these peaks can be controlled. The Zeeman sublevels are not considered in our three-level calculation model. In Fig. 3(a), there is a main peak and several subpeaks indicated by filled circles (\bullet). These subpeaks were generated by the modulation and were reproduced in the experiment as shown in Fig. 3(c). However, the second-order subpeaks ($\bullet 2$) were larger than the first-order subpeaks ($\bullet 1$) in contrast to the calculation result. This difference was due to the residual amplitude modulation (RAM) of the VCSEL.^{13,14} By comparing Figs. 3(c) and 3(d), we clearly confirmed the widening of the LR. The measured LR with FM was limited by the noise and was 6.8 kHz . On the other hand, the measured LR with PM was limited by not the noise but the subpeaks generated by the modulation. For the sake of comparison between the deviation of the LO frequency and LR, the fractional LR (FLR) is defined as

$$\text{FLR}_{\text{PM}} = \frac{\text{LR}_{\text{PM}}}{f_{\text{hfs}}}, \quad (3)$$

where f_{hfs} is the hyperfine splitting frequency between ground states. In Figs. 3(a) and 3(c), the LR (FLR) reached 200 kHz (29.3 ppm) and 100 kHz (14.6 ppm), respectively. The theoretical LR_{PM} is equal to twice the modulation frequency $2f_{\text{mod}}$. The LR in the experiment was reduced by the Zeeman sublevels, which can be tuned via the bias magnetic field.

Figure 4 shows the Allan deviations of the CPT atomic clock using PM and FM. The frequency stability of the LO was 6.2×10^{-11} at 1 s. The short-term stability is mainly limited by the laser FM noise, which decreases at higher Fourier

frequencies.¹⁵ Since the PM method allows signal detection at higher frequencies where the laser FM noise is relatively lower, an improved fractional frequency stability was obtained by the PM method.

In conclusion, the PM method was applied to the detection of the CPT resonance to expand the locking range without broadening the linewidth. Error signals using the PM method were numerically calculated by a time-domain analysis based on a density matrix, and they were compared with those using the conventional FM method. As a result, the PM method can provide a 29-fold wider locking range than the FM method. It was found that the PM method is effective in detecting the CPT resonance similarly to the two-level system in optical spectroscopy. Furthermore, the PM method was applied to a desktop-scale atomic clock employing an ^{87}Rb vapor cell and a VCSEL. Unlike the numerical expectation, the expansion of the locking range was limited by the Zeeman sublevels. The measured fractional locking range was 14.6 ppm , which was 14.6 times wider than that measured using the FM method. Frequency stability was also improved by using the PM method.

The wider locking range obtained with our method relaxes a constraint in the deviation of the LO frequency, which may contribute to the reduction in the size, cost, and power consumption of the CPT clock. Furthermore, note that the wider locking range reduces the settling time of the feedback to engage the stabilization. It realizes not only the robustness of the frequency lock but also intermittent operation for the battery operated devices in the future.

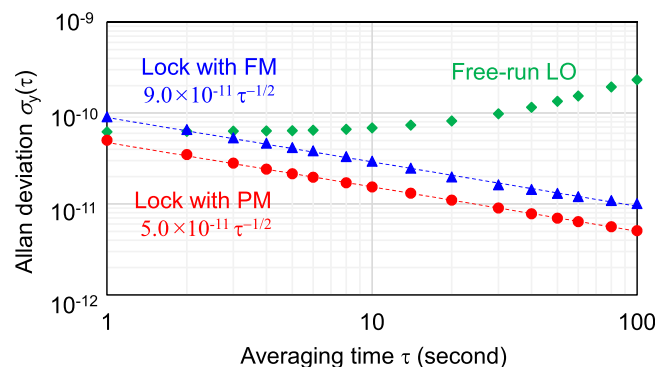


FIG. 4. Allan deviations: the circular and triangular dots are those for the CPT atomic clock with PM and FM, respectively. The square dots are those for free-run LO.

We wish to thank Hiroshi Ishijima, Junichi Komuro, and Kohta Kido for their kind support of our experiment. This work was supported by a Grant-in-Aid for Scientific Research (C) (Grant No. JP17K06483) from Japan Society for the Promotion of Science (JSPS) KAKENHI. Y.Y. was supported by a Grant-in-Aid for Young Scientists (B) (Grant No. JP17K14697). M.K. was supported by a Grant-in-Aid for Scientific Research (C) (Grant No. JP16K05500), a Grant-in-Aid for Scientific Research (B) (Grant No. JP17H02881), and a Grant-in-Aid for Exploratory Research (Grant No. 15K13545) from JSPS.

- ¹S. Knappe, V. Shah, P. D. D. Schwindt, L. Hollberg, J. Kitching, L.-A. Liew, and J. Moreland, "A microfabricated atomic clock," *Appl. Phys. Lett.* **85**, 1460–1462 (2004).
- ²R. Lutwak, "The chip-scale atomic clock-recent developments," in *Proceedings of 2009 Joint Conference of the IEEE International Frequency Control Symposium and the European Frequency and Time Forum* (IEEE, 2009), pp. 573–577.
- ³G. C. Bjorklund, "Frequency-modulation spectroscopy: a new method for measuring weak absorptions and dispersions," *Opt. Lett.* **5**, 15–17 (1980).
- ⁴J. M. Supplee, E. A. Whittaker, and W. Lenth, "Theoretical description of frequency modulation and wavelength modulation spectroscopy," *Appl. Opt.* **33**, 6294–6302 (1994).
- ⁵E. D. Black, "An introduction to Pound–Drever–Hall laser frequency stabilization," *Am. J. Phys.* **69**, 79–87 (2001).

- ⁶R. Wynands and A. Nagel, "Precision spectroscopy with coherent dark states," *Appl. Phys. B* **68**, 1–25 (1999).
- ⁷Y. Yano, W. Gao, S. Goka, and M. Kajita, "Theoretical and experimental investigation of the light shift in Ramsey coherent population trapping," *Phys. Rev. A* **90**, 013826 (2014).
- ⁸Y. Yano, S. Goka, and M. Kajita, "Estimation of the light shift in Ramsey-coherent population trapping," in *Proceedings of 2015 Joint Conference of the IEEE International Frequency Control Symposium and the European Frequency and Time Forum* (IEEE, 2015), pp. 162–166.
- ⁹V. I. Yudin, A. V. Taichenachev, M. Y. Basalaev, and D. V. Kovalenko, "Dynamic regime of coherent population trapping and optimization of frequency modulation parameters in atomic clocks," *Opt. Express* **25**, 2742–2751 (2017).
- ¹⁰I. Ben-Aroya, M. Kahanov, and G. Eisenstein, "Multi-field frequency modulation spectroscopy," *Opt. Express* **16**, 6081–6097 (2008).
- ¹¹G. A. Pitz, A. J. Sandoval, T. B. Tafoya, W. L. Klennert, and D. A. Hostutler, "Pressure broadening and shift of the rubidium D_1 transition and potassium D_2 transitions by various gases with comparison to other alkali rates," *J. Quant. Spectrosc. Radiat. Transfer* **140**, 18–29 (2014).
- ¹²S. Bize, Y. Sortais, M. Santos, C. Mandache, A. Clairon, and C. Salomon, "High-accuracy measurement of the ^{87}Rb ground-state hyperfine splitting in an atomic fountain," *Europhys. Lett.* **45**, 558 (1999).
- ¹³E. A. Whittaker, M. Gehrtz, and G. C. Bjorklund, "Residual amplitude modulation in laser electro-optic phase modulation," *JOSA B* **2**, 1320–1326 (1985).
- ¹⁴X. Zhu and D. T. Cassidy, "Modulation spectroscopy with a semiconductor diode laser by injection-current modulation," *JOSA B* **14**, 1945–1950 (1997).
- ¹⁵J. Kitching, H. Robinson, L. Hollberg, S. Knappe, and R. Wynands, "Optical-pumping noise in laser-pumped, all-optical microwave frequency references," *JOSA B* **18**, 1676–1683 (2001).